# A fundamental study of combined free and forced convective heat transfer from a vertical plate followed by a backward step

Received March 1997
Accepted March 1998

Koki Kishinami, Hakaru Saito, Jun Suzuki and Ahmed Hamza H. Ali
*Department of Mechanical Systems Engineering, Muroran Institute of Technology, Hokkaido, Japan*
Hisashi Umeki
*Smex. Ltd, Muroran, Hokkaido, Japan and*
Noriyuki Kitano
*Hitachi Zosen Ltd, Konohana, Osaka, Japan*

## Nomenclature

d = height of the backward-facing step
L = length of upper vertical plate as characteristic length
h = heat transfer coefficient based on temperature difference in $(t_w-t_\infty)$
t = fluid temperature
U,V = dimensionless vertical and transverse velocities defined by equation (1)
X,Y = dimensionless vertical and transverse coordinates defined by equation (1)
T = dimensionless temperature defined by equation (1)
Suffix w = wall, ∞: surroundings
$Gr_L$ = Grashof number based on L and temperature difference in $(t_w-t_\infty)$
$Re_L$ = Reynolds number based on L and free stream velocity $U_\infty$
Pr = Prandtl number
$Nu_L$ = local Nusselt number defined by equation (7)
$\overline{Nu_L}$ = mean Nusselt number defined by equation (8)
$\overline{Nu_L}Re_L^{1/2}$ = heat transfer characteristics
$\tau^*$ = dimensionless time defined by equation (1)
$\Psi$ = dimensionless streamline function defined by equation (2)
$\Omega$ = dimensional vorticity defined by equation (3)

## 1. Introduction

Combined forced and free convective heat transfer coupled with thermal conduction and separated recirculation flow has been becoming important in recent years, both in academic and in practical fields (Kishinami *et al.*, 1995; Tsou *et al.*, 1991). Problems with flows similar to those considered here have become the subjects of considerable interest in several technological

One of the authors, Hakaru Saito, died in February 1996.

International Journal of Numerical Methods for Heat & Fluid Flow
Vol. 8 No. 6, 1998, pp. 717–736.

applications, such as flow encountered in heat exchangers, electronic semiconductor devices and many other manufacturing systems.

Two-dimensional flow passing over a backward-facing step, which represents one of the simplest geometries for creating separation and reattachment of the recirculating shear flow, has been studied extensively. However, the combined convective flow past a backward-facing step strongly depends on the interaction between the buoyancy and inertia forces. For example, starting flow and heat transfer downstream of a backward-facing step in high velocity, in steady state, was reported by Tsuo *et al.* (1991). Also, steady natural convection heat transfer from a vertical plate followed by a backward-facing step by Saito *et al.* (1995). Most of the papers presented up to now have treated the heat transfer in similar cases by considering the pure natural/forced convection, and have paid little attention to the case of the combined convection flow in which peculiar heat transfer may occur (Kishinami *et al.*, 1995).

The objective of the present paper is to investigate the transient combined forced and free laminar convective heat transfer from a vertical plate with backward-facing step by means of numerical and experimental approaches. This investigated model was limited to the case of the buoyancy and inertia forces in the same direction and the induced starting flow taking place in the separation and reattachment after the step region. The research conditions presented here cover the range of characteristic lengths from the leading edge to the step of L = 80-160mm, the step geometrical factor, the ratio of L to the step height of d, d/L = 0.2-0.5, difference in temperature between the convective isothermal surface and surroundings $\Delta t$ = 15-50°C and the free stream velocity of $U_\infty$ = 0.2-0.6m/s. Numerical calculations for various combinations of the Grashof number $Gr_L$, Reynolds number $Re_L$ and geometry factor d/L are carried out for transient laminar, combined forced and free convective flow by means of the hybrid and Donar-cell up-wind difference scheme. Experimental corroboration is provided by the result of the Mach-Zehnder interferometer and the measurement of temperature distribution with 0.1mm $\phi$ C-C thermocouple under the same conditions as mentioned above. Transient/steady state heat transfer behavior obtained by the numerical calculations and observed in some experiments such as Nusselt number and velocity/temperature distributions and streamline fields are discussed to clarify the effects of the parameters such as $Gr_L$, $Re_L$ and d/L.

Special attention is given to the periodically fluctuating behavior, similar to the self-excited oscillation, of the mixed convection at the specific range of the generalized coupling parameter $Gr_L/Re_L^2$.

## 2. Physical model and numerical procedure

The schematic diagrams for the physical and numerical model of forced-free mixed air convection under consideration is shown in Figures 1 and 2, together with the boundary conditions. These figures show that the separated flow and recirculation take place on the step region B-C and downstream region C-D. The vertical isothermal heating plate is located in the opposite direction to the

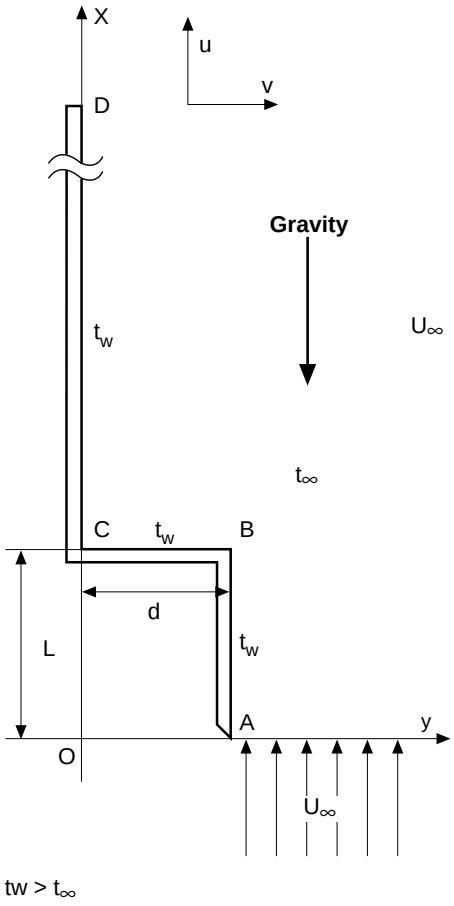


**Figure 1.**
Physical model

gravity and set up in the parallel flow of the free stream velocity $U_\infty$. The x- and y-axes originated from the leading edge are taken as the vertical and transverse coordinates.

The outline of the separating recirculated convective flow is shown in Figure 2. At the beginning of the surface heating under the constant free stream velocity $U_\infty$ an initial boundary layer flow (1) passes around the corner of the step, creating a free shear layer (3) and a recirculating region (2) developed on the step and redeveloping region (4) on the downstream vertical plate. A dividing streamline was done to separate the downstream flowing zone and the recirculation region, and to intersect the downstream wall. The intersecting point is considered as the reattachment point. After this point, the downstream flow was redeveloped into a boundary layer type flow (Saito *et al.*, 1995; Tsuo *et al.*, 1991).

The combined forced and free convective heat transfer is treated as transient, laminar flows developed by the cooperation of the buoyancy and inertia forces

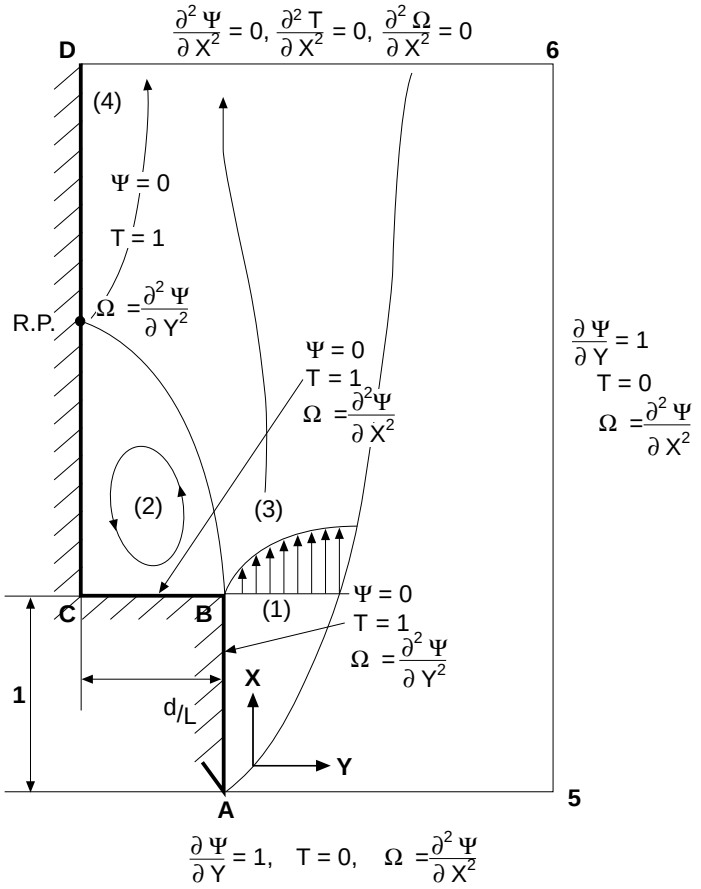


**Figure 2.**
Numerical model with boundary conditions

over the isothermal heated vertical plate, including the vortex flow in the recirculating region near the step.

*Governing equations*

The following dimensionless variables, commonly used for the transient combined forced and free convection, can be defined by taking the upper vertical plate length of L and the free stream velocity of $U_\infty$ as the characteristic length and velocity:

$$X = \frac{x}{L}, \quad Y = \frac{y}{L}, \quad U = \frac{u}{U_\infty}, \quad V = \frac{v}{U_\infty}, \quad T = \frac{t - t_\infty}{t_w - t_\infty},$$

$$\tau^* = \frac{\tau U_\infty}{L}, Pr = \frac{\nu}{\alpha}, Re_L = \frac{U_\infty L}{\nu}, Gr_L = \frac{g\beta(t_w - t_\infty)L^3}{\nu^2} \tag{1}$$

where the nondimensional time $\tau^* = \tau U_\infty/L$ is based on the assumption of $Re_L > 1$ for the forced convection system (Patanker, 1980; Roache, 1976). The dimensionless stream function $\Psi$ and vorticity $\Omega$ are defined as follows by applying the above variables (1):

$$\Psi = \frac{\psi}{U_\infty L} : \; U = \frac{\partial \Psi}{\partial Y}, \; V = -\frac{\partial \Psi}{\partial X} \tag{2}$$

$$\Omega = \frac{L\omega}{U_\infty} : \quad \Omega = \frac{\partial^2 \Psi}{\partial X^2} + \frac{\partial^2 \Psi}{\partial Y^2} \tag{3}$$

The energy and vorticity transport equations are given in the following dimensionless forms in the same manner as above:

$$\frac{\partial T}{\partial \tau^*} + U\frac{\partial T}{\partial X} + V\frac{\partial T}{\partial Y} = \frac{1}{Re_L Pr}\left(\frac{\partial^2 T}{\partial X^2} + \frac{\partial^2 T}{\partial Y^2}\right) \tag{4}$$

$$\frac{\partial \Omega}{\partial \tau^*} + U\frac{\partial \Omega}{\partial X} + V\frac{\partial \Omega}{\partial Y} = \frac{Gr_L}{Re_L^2}\frac{\partial T}{\partial Y} + \frac{1}{Re_L}\left(\frac{\partial^2 \Omega}{\partial X^2} + \frac{\partial^2 \Omega}{\partial Y^2}\right) \tag{5}$$

The local Nusselt number $Nu_L$ on the convective surface of the wall can be expressed as follows, based on the difference in temperature between the surface and the surroundings:

at the vertical surface $$Nu_L = \frac{hL}{\lambda} = -\left.\frac{\partial T}{\partial Y}\right|_{Y=0,d/L} \tag{6}$$

at the step surface $$Nu_L = \frac{hL}{\lambda} = -\left.\frac{\partial T}{\partial X}\right|_{X=1} \tag{7}$$

Average means Nussel $\overline{Nu_L}$ from the leading edge to the X location, including step region, can be expressed as follows.

$$\overline{Nu_L} = \frac{1}{X}\int_0^X Nu_L dX + \frac{1}{d/L}\int_0^{d/L} Nu_L dY \tag{8}$$

*Outline of numerical solution technique*

The governing equations of the energy and vorticity transportation are parabolic regarding time $\tau^*$. Hence, the solution for the problem can be marched in time and in the downstream direction based on a given initial distribution of $U_\infty$, $\Psi$ and T. Triple integrations of the equations (4) and (5) with respect to $\tau^*$, X and Y based on the control volume integration for the interval time $\tau^* - \tau^* + \Delta\tau^*$ and spaces $X - X + \Delta X$, $Y - Y + \Delta Y$ can be derived by using Crank-Nicolson

implicit scheme (Patanker, 1980). In the derivation of the scheme the values of the weighting factor f = 0.7 (weightings in implicit and explicit terms are 0.7 and 0.3, respectively) were chosen in order to obtain the more exact results of the calculation by employing a very small time step $\Delta\tau^*$. Here, the finite discretization approximations were performed by the upstream difference in the convection terms and the central difference in the diffusion terms. The resulting system of the discretized equations can be solved by a Gauss Seidel Iteration at every time step marching.

In this calculation to improve the accuracy of the numerical results, the hybrid scheme was employed to minimize the effect of the artificial viscosity caused from the upstream difference scheme (Roache, 1976). The mesh size of 70 $\times$ 70 was normally used in addition to the adoption of the high grid-density near the wall and the leading edge (Kishinami *et al.*, 1995).

## 3. Experimental apparatus and procedure

Figure 3 shows an outline of the experimental apparatus. The apparatus was subdivided into two components; one is the test section of the convection plate with backward-facing step, and the other the open type of a wind tunnel to make a forced convection and the Mach-Zehnder interferometer to measure the temperature fields. The convection test plate comprised the upper vertical plate with length of L = 80mm, the backward-facing step with height of d = 10-40mm and the downstream vertical plate with length of 480mm. The convection surfaces are made of 5mm thick aluminum plate and isothermally heated from the rear by an electrical heater (Nichrome wire of 0.26mm $\phi$) set in a phenol resin holder plate with thickness of 10 mm, and controlled at a heating temperature between 35-70°C within the accuracy of 0.3°C.

A low velocity an open type wind tunnel was installed at the bottom of the vertical plate. The free stream velocity $U_\infty$ at the outlet of the wind tunnel was regulated from 0.2-0.6m/s by a 500mm diameter propeller driven by a 150W inverter controlled motor (Kishinami *et al.*, 1995). The forced air was rectified through the three stages honeycomb with dimensions 260 $\times$ 300 $\times$ 30mm (hole diameter 3mm $\phi$), guide vanes to change the flow direction and a throttling passage.

The isothermal distribution in the boundary layer and the recirculating region were measured both by the interferogram of Mach-Zehnder interferometer and by a 0.1mm $\phi$ C-C thermocouple probe link to a PC-98 computer, and also the free stream velocity $U_\infty$ by a thermistor anemometer.

## 4. Results and discussion

### *Ordinary behaviors of combined convection*

Figures 4 and 5 show the temperature field (isothermal line) for the step geometry factor of d/L = 0.2 and 0.5. These results are obtained by the interferogram (left) of the Mach-Zehnder interferometer and the numerical results (right) under the same condition of $Re_L$ = 1,027 ($U_\infty$ = 0.2m/s) and $Gr_L$ = $3.17 \times 10^6$ ($\Delta t$ = 45°C). The streamline distribution obtained by numerical

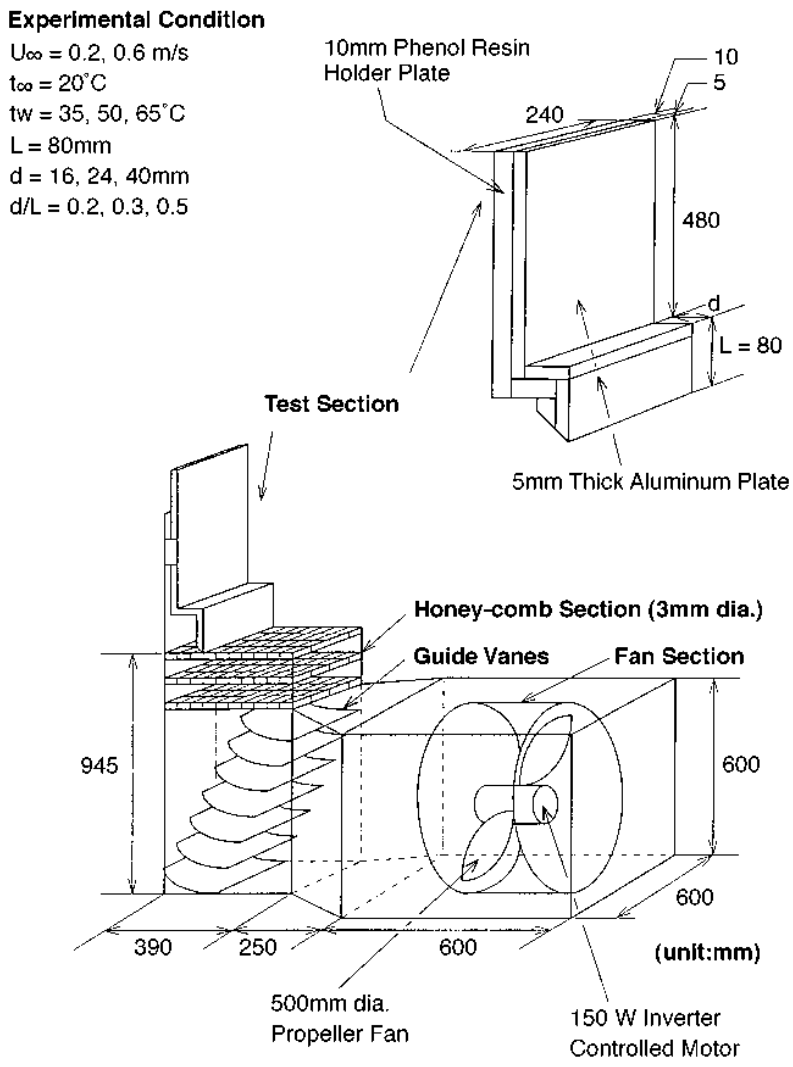


**Figure 3.**
Experimental apparatus

calculation is expressed in Figure 6 for the same condition as above. As clearly seen in these figures, the experimental isothermal temperature contours are found to be in good agreement with those of the numerical results. The combined forced and free laminar flow is recognized to develop from the leading edge (A) to the rear edge (B) on the upper vertical plate. After the step edge (B) the flow changes its direction toward the downstream vertical wall and separates to two regions into the downstream flowing fluid and the recirculating fluid. On the step surface (B-C) the flow forms a recirculating region which becomes an enlargement of its territory in proportional to the step geometry factor of d/L as shown Figure 6. For the cases of high values d/L, it is

$L = 0.08[m]$, $U\infty = 0.2[m/s]$, $tw = 65[^{\circ}C]$
$[Re_L = 1027, Gr_L = 3.17 \times 10^6]$

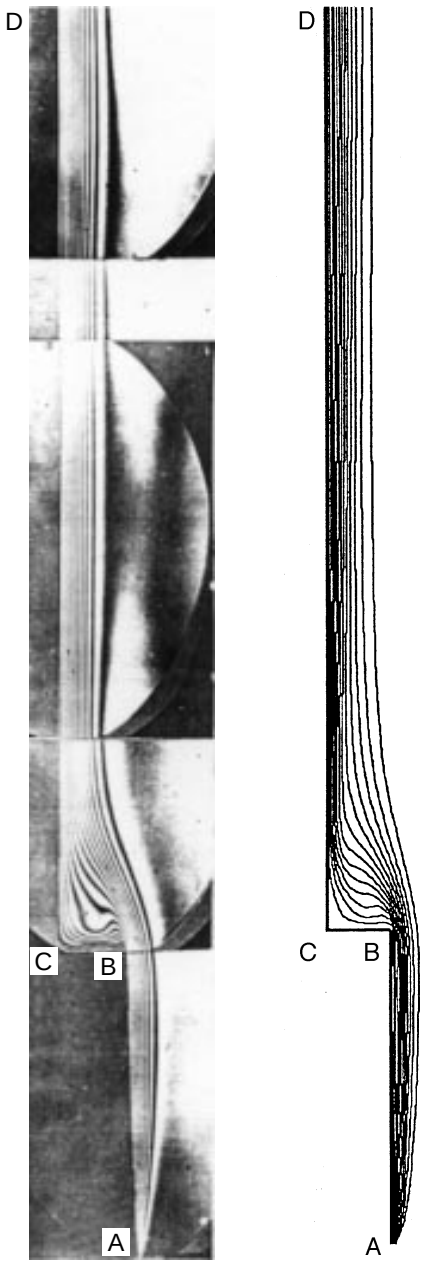


d/L = 0.2

**Figure 4.**
Result of isothermal contour for d/L = 0.2

$L = 0.08[m]$, $U\infty = 0.2[m/s]$, $tw = 65[^{\circ}C]$

$[Re_L = 1027, Gr_L = 3.17 \times 10^6]$

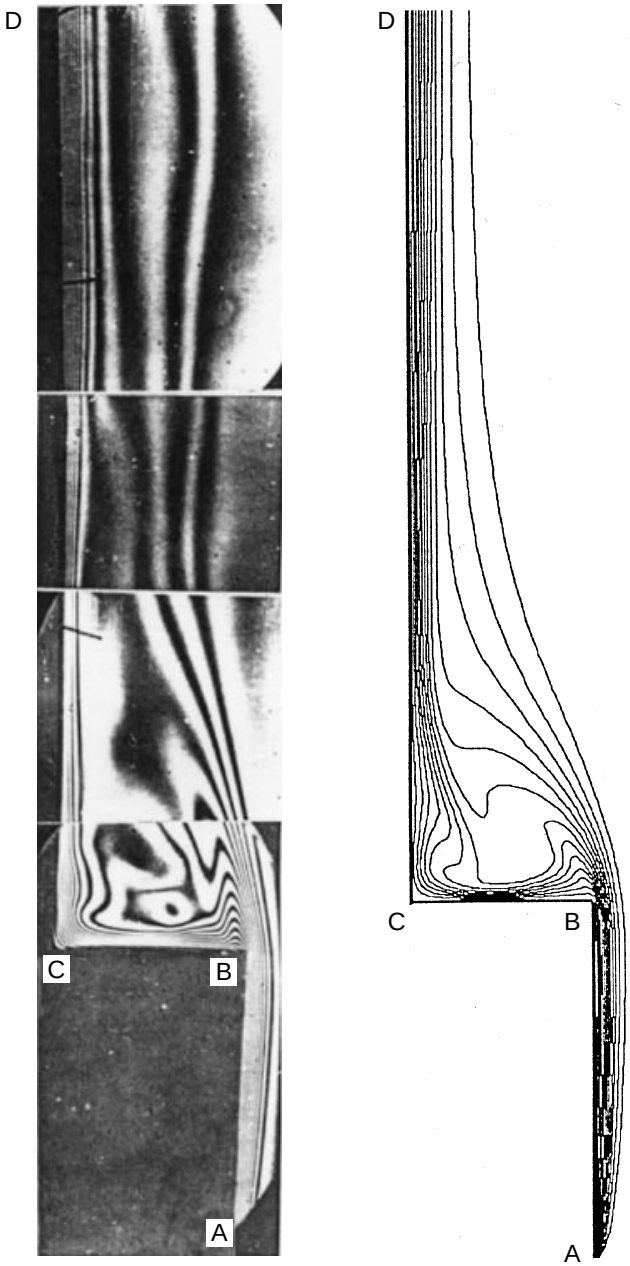


d/L = 0.5

**Figure 5.**
Result of isothermal contour for d/L = 0.5

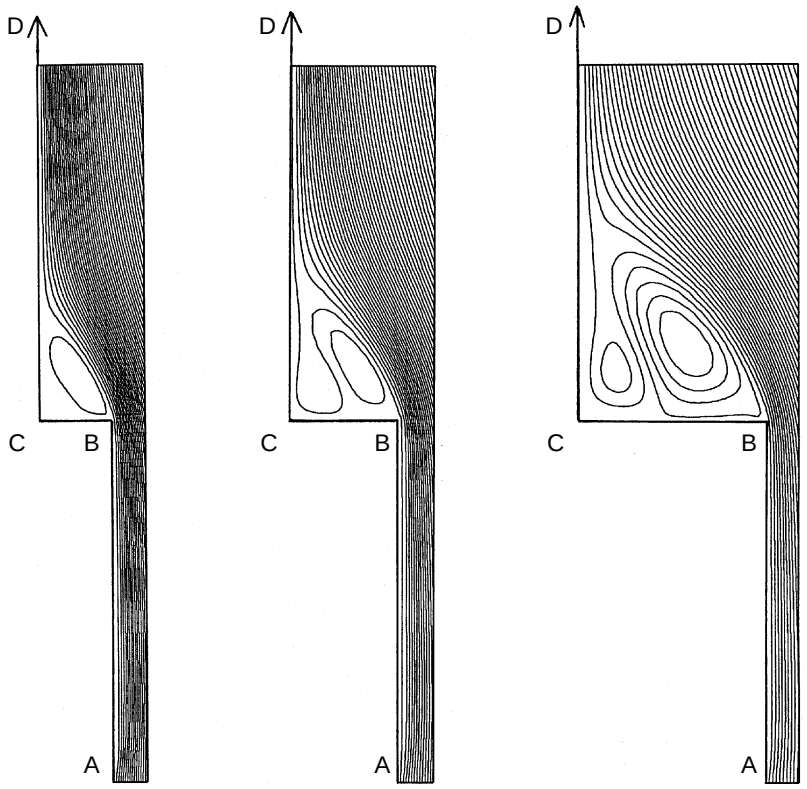


**(a)** d/L = 0.2 **(b)** d/L = 0.3 **(c)** d/L = 0.5

$L = 0.08[m]$, $U\infty = 0.2[m/s]$, $tw = 65[^{\circ}C]$
$[Re_L = 1027, Gr_L = 3.17 \times 10^6]$

**Figure 6.**
Result of streamline for d/L = 0.2-0.5

found that a weak rotating secondary vortex flow in the clockwise direction appears gradually on the inner corner of the step (C) in addition to the presence of a main vortex flow rotating in the opposite direction on the corner side (B). The boundary flow passing over the recirculating region reattaches to the downstream vertical wall and makes the redevelopment of the boundary layer along the surface. The temperature field on the step region becomes very complex according to the step geometry and the interaction between the inertia and buoyancy forces. That is in general, the temperature gradient becomes very low at the inner corner edge (C) and high at the central region of the step.

Figure 7 shows the local Nusselt number $Nu_L$ in dimensionless form of local heat transfer coefficient with the geometry factor of d/L = 0.2 and 0.5, corresponding to the same condition as mentioned above. In Figure 7 the bold

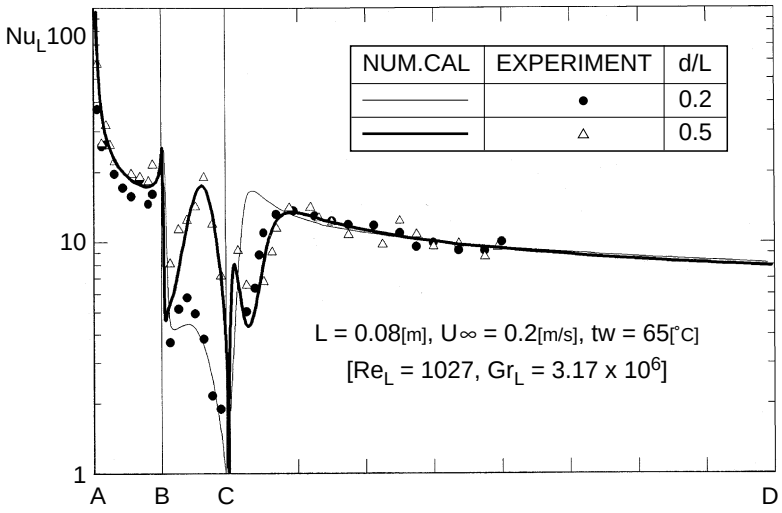


**Figure 7.**
Local Nusselt number $Nu_L$ for d/L = 0.2 and 0.5

and fine solid lines represent the numerical results of $Nu_L$ for the d/L = 0.2 and 0.5, while the symbols Δ and ● indicate the experimental data for the same conditions. The section (B-C) of the step region was treated by dividing the d/L, subsequently the section is always a unit instead of the dimensionless section of the d/L. Comparing the numerical data to experiment in Figure 7, both results are seen to be in good agreement with each other. As a whole, the behavior of the local Nusselt number $Nu_L$ is very close to the case of the single isothermal plate, except in the vicinity of the step. However, to pay attention to the effect of d/L on the $Nu_L$ near the step region, the large difference in the $Nu_L$ is recognized depending upon the geometry factor as seen in bold and fine solid lines. The local Nusselt number $Nu_L$ on the central region of the step is recognized to considerably increase in its value with increasing the geometry factor of d/L. This is caused by the presence of the two separated vortices with the counterclockwise and opposite directions rotating in the recirculation region shown in Figure 6 (C) for the d/L = 0.5. It is generally accepted that the heat transfer enhancement occurs at the position of the surface which the fluids are impinging on. Therefore, the position of the maximum values of $Nu_L$ on the downstream vertical wall (C-D) is interpreted as a result of the reattachment of the downstream boundary flow (Saito *et al.*, 1995). The reattachment point is found to have the tendency toward moving downstreamward when the d/L increases, which causes the enlargement of the recirculating region as shown in the figures.

*Effects of buoyancy/inertia forces on combined convection*

Figures 8 and 9 represent the local Nusselt number $Nu_L$ and the velocity vector diagrams for the Grashof number $Gr_L = 1.03 \times 10^6$ and $3.17 \times 10^6$ ($\Delta t$ = 15 and 50°C) under the constant Reynolds number $Re_L$ = 1,027 ($U_\infty$ = 0.2m/s) and the

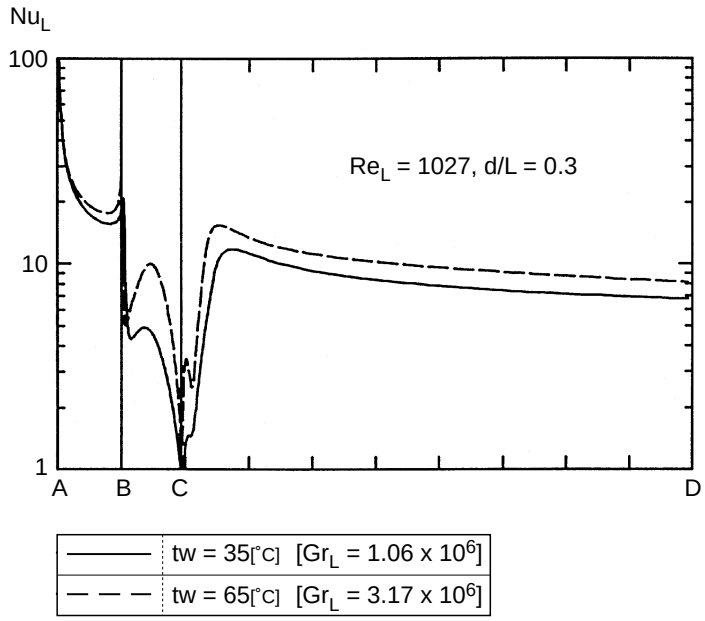


**Figure 8.**
Local Nusselt number $Nu_L$ depending on $Gr_L$ at constant $Re_L$ = 1,027 for d/L = 0.3

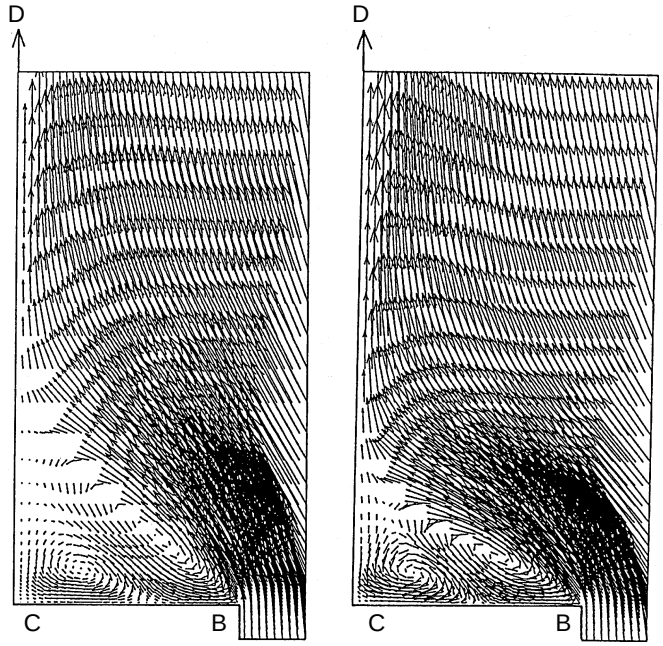


**(a)** $Gr_L = 1.06 \times 10^6$ **(b)** $Gr_L = 3.17 \times 10^6$

$Re_L$ = 1027 d/L = 0.3

**Figure 9.**
Velocity vector depending on $Gr_L$ at constant $Re_L$ = 1,027 for d/L = 0.3

geometry factor of d/L = 0.3. For the condition of the low inertia force ($U_\infty$ = 0.2m/s), it is understood that the effect of the buoyancy on the $Nu_L$ yields the 20-40 percent enhancement of heat transfer after the step, which becomes remarkable in the downward region, as the result of the increase in the velocity near the wall. The buoyancy effect on the velocity fields is seen to act on the reduction of the recirculation region and to strengthen the velocity near the wall and the two separated vertexes on the step. Subsequently, the heat transfer enhancement due to the buoyancy force can be expected in the downward region and in the central step region.

In turn, Figures 10 and 11 represent the local Nusselt number $Nu_L$ and the streamline diagrams for the Reynolds number $Re_L$ = 1,027 and 3,081 ($U_\infty$ = 0.2 and 0.6m/s) under the constant Grashof number $Gr_L = 3.17 \times 10^6$ ($\Delta \mathbf{t}$ = 50°C) and a geometry factor of d/L = 0.3. Under the constant effect of the buoyancy, the influence of the free stream velocity $U_\infty$ on the $Nu_L$ is recognized to make a heat transfer enhancement on the upper region while the enhancement is not so much on the downward region. The effect of the free stream velocity $U_\infty$ on the velocity field is seen to strongly act on the enlargement of the recirculating region, in which the dull two separated vortices produce a low $Nu_L$ on the region near the inner corner (C) and shift the reattachment point downward.

As a result of the above discussion, it is concluded that the effects of the buoyancy/inertia forces play an important role in acting on the reduction/enlargement of the recirculating region, and that the geometry factor d/L operates in the same manner as the inertia force.

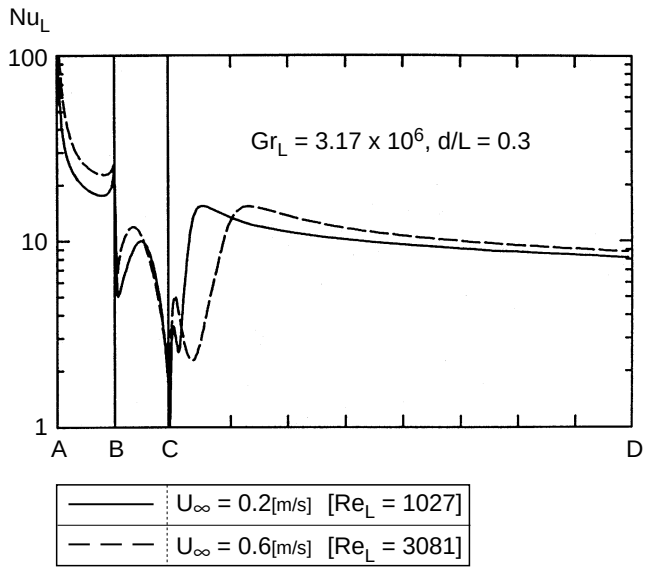


**Figure 10.**
Local Nusselt number $Nu_L$ depending on $Re_L$ at constant $Gr_L = 3.17 \times 10^6$ for d/L = 0.3

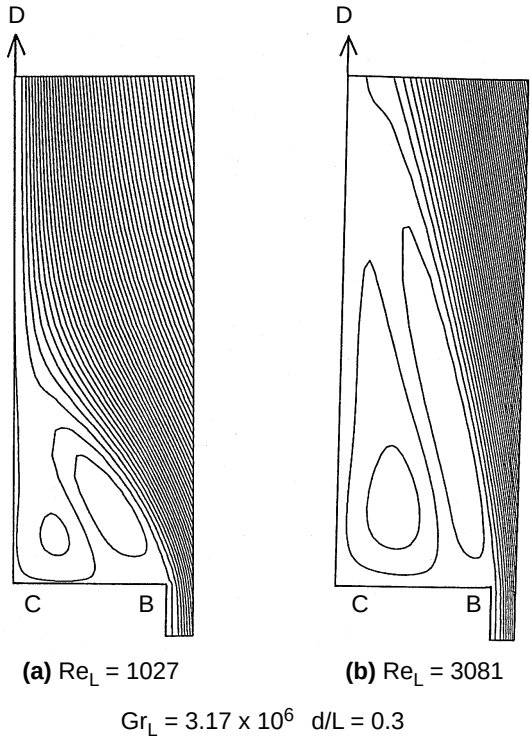


**Figure 11.**
Streamline depending on $Re_L$ at constant $Gr_L = 3.17 \times 10^6$ for $d/L = 0.3$

*Heat transfer characteristics* $\overline{Nu_L}/Re_L^{1/2}$

Usually, the dimensionless coupling number of $Gr_L/Re_L^2$ is the most important parameter to explain the behavior of the combined forced and free convection heat transfer (Kishinami *et al.*, 1995). Then, the relation of the mean Nusselt number $\overline{Nu_L}$ from the leading edge to the vertical location X = 4.0 and the coupling parameter $Gr_L/Re_L^2$ is introduced in this problem.

Figure 12 shows the relationship between the heat transfer characteristics $\overline{Nu_L}/Re_L^{1/2}$ the coupling parameter $Gr_L/Re_L^2$ of this convection for the cases of the geometry factor of d/L = 0.1, 0.2 and 0.3 as a parameter. For the mixed convection range, it can be concluded that the heat transfer characteristics $\overline{Nu_L}/Re_L^{1/2}$ are sharply dependent on the coupling parameter $Gr_L/Re_L^2$ and the geometry factor d/L within the limiting condition of the present research. However, the behavior of $\overline{Nu_L}/Re_L^{1/2}$ is recognized to have a different mode from the case of the single isothermal plate (1) due to the presence of the recirculating region near the step with the increase in the d/L. Furthermore, the considerable transient unstable behavior of the $Nu_L$ is recognized at the specified range of $Gr_L/Re_L^2$ = 0.4-0.6 for the geometry factor of D/L = 0.5.

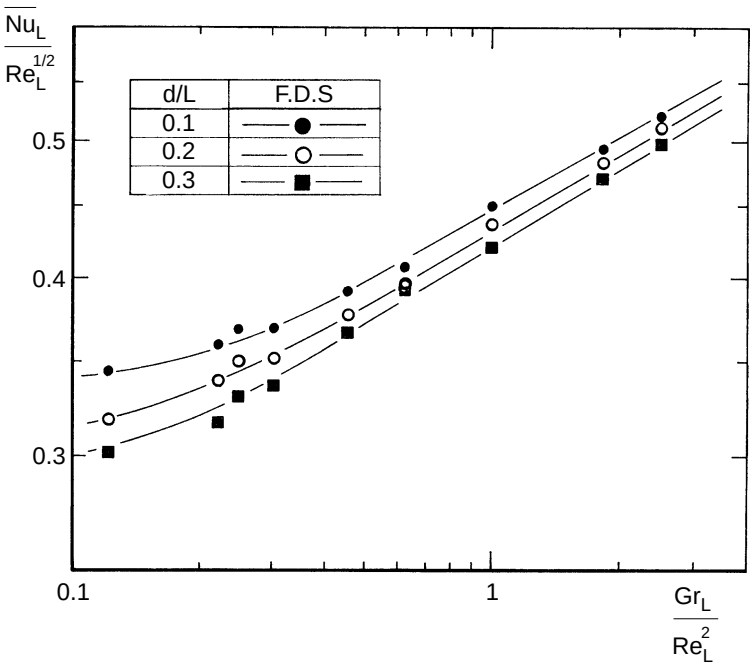


**Figure 12.**
Relationship between mean heat transfer characteristics $\overline{Nu_L}/Re_L^{1/2}$ and coupling nondimensional number $Gr_L/Re_L^2$

*Unsteady transient behavior of combined convective heat transfer*

Figure 13 represents the local Nusselt number variation obtained by numerical calculation for the case of $Gr_L/Re_L^2 = 0.59$ and d/L = 0.5, Reynolds number $Re_L$ = 1,444 ($U_\infty$ = 0.3m/s) and Grashof number $Gr_L = 1.24 \times 10^6$ ($\Delta t$ = 20°C) as the time elapsed $\tau$ = 30.00-30.75 sec. with the interval 0.25 sec. after the starting of the heating. From Figure 13 stable steady state heat transfer can be seen on the upper vertical plate and on the step region. However, the transient unstable fluctuating heat transfer mode is widely recognized at the transient zone (X = 1.8-3.8) near the region of maximum $Nu_L$ on the downstream vertical plate, which is considered as a reattachment point. Hence, it is necessary to check the streamline diagram causing the unstable fluctuation behavior of $Nu_L$.

Figure 14 illustrates the three typical patterns of the streamline diagram for the cases of $Gr_L/Re_L^2 = 0.11$, 0.59 and 3.34, respectively. It is generally interpreted that the coupling parameter of $Gr_L/Re_L^2 = g\beta(t_w-t_\infty)L/U_\infty^2$ represents the ratio of the buoyancy and the inertia forces. Therefore, the case of the low/high value of the parameter corresponds with the predomination of the forced/natural convection over the flow field. For the case (a) of $Gr_L/Re_L^2$ = 0.11 which is under the domain of the forced convection, the vortex flow with rotating clockwise direction seems to be dominant in the enlarged recirculating region. On the contrary for the case (c) of $Gr_L/Re_L^2 = 3.34$ under the domain of the natural convection, the vortex flow with rotating counterclockwise direction seems to be remarkable in the reduced recirculation region. For both cases the

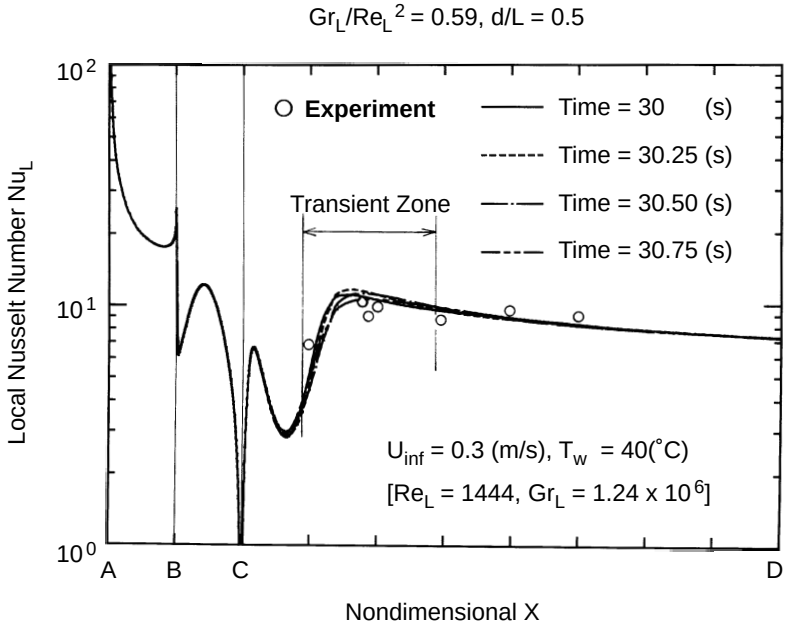


**Figure 13.**
Transient local Nusselt number $Nu_L$ for d/L = 0.5 at $Gr_L/Re_L^2$ = 0.59

unstable fluctuating behavior of $Nu_L$ cannot be observed even in the reattachment zone. For the case (b) of $Gr_L/Re_L^2$ = 0.59 where the effects of the forced and natural convection are comparable, i.e. the coexistence of the two separated vortices rotating in the opposite directions with each other, the unsteady fluctuating behaviors of the streamline and temperature contours are recognized near the reattachment point of the downstream vertical wall. These fluctuations are likely to collapse the balance between the natural and forced convection. This causes the transient unstable flow similar to the self-excited oscillation, i.e. the unsteady fluctuating convection heat transfer. From the observation, it is revealed that such a fluctuating local heat transfer behavior occurs only near the reattachment point within the limiting range of the generalized coupling parameter, $0.3 < Gr_L/Re_L^2 < 2.5$.

Figure 15 represents the experimental results of the transient behaviors of the temperature boundary layer for the condition of $Gr_L/Re_L^2$ = 0.59, d/L = 0.5 obtained by a 0.1mm $\phi$ C-C thermocouple inserted in the position of Y = 0.0125, 0.0625, 0.1125 and 0.1652 at the location of X = 2.8. Corresponding lower diagram shows the numerical results of the velocity and temperature distributions, where the temperature is compared with the experimental result of the average values of the above transient measured data. From the Figure, it is clear that the fluctuation behaviors are strongly recognized at the core of the field near the reattachment point although the numerical prediction is not so clear as the experiment.

Figure 16 illustrates the time history of the fluctuation of local heat transfer $Nu_L$ near the reattachment point X = 2.6-3.0 for the specified condition of the

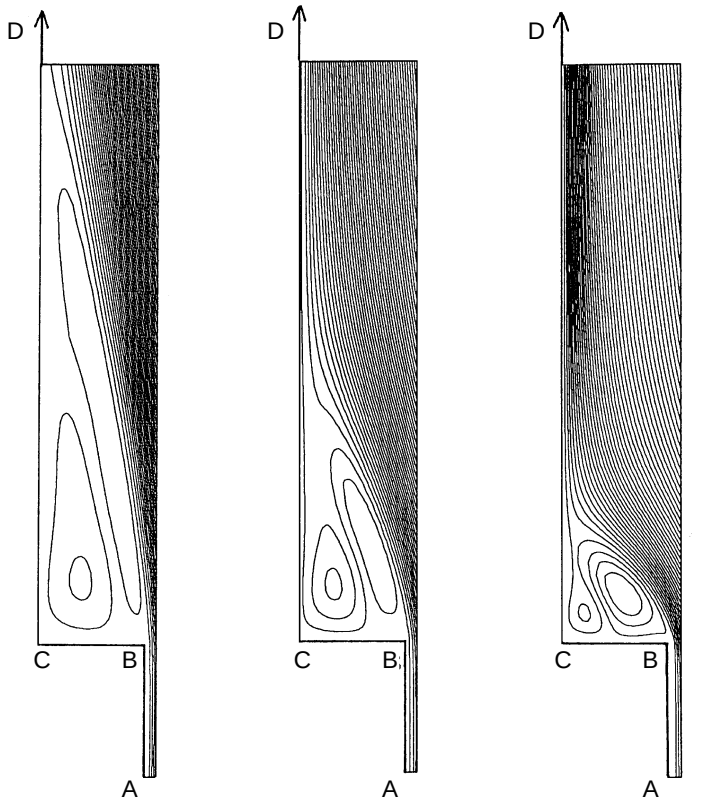


**Figure 14.**
Patterns of streamline for d/L = 0.5 at $Gr_L/Re_L^2$ = 0.11, 0.59 and 3.34

coupling number of $Gr_L/Re_L^2 = 0.59$ and the geometry factor of d/L = 0.5. The components $Gr_L$ and $Re_L$ are changeable, keeping the value of the coupling parameter constant, under the constant free stream velocity $U_\infty$ = 0.3m/s. For the case (a) of L = 0.08m corresponding to the same condition as above, the frequency is observed as about 1 sec with a small amplitude, for the case (b) of L = 0.1m the frequency is about 1.25 sec with a moderate amplitude, and for the case (c) of L = 0.16m the frequency is about 2 sec with a high amplitude. It seems that the amplitude and frequency are proportional to the order of the length L or Reynold number $Re_L$ although the local heat transfer characteristics $\overline{Nu_L}/Re_L^{1/2}$ are nearly constant within the X range of 0.26-0.30.

It is concluded that the unsteady fluctuating heat transfer behavior of $Nu_L$, which is very similar to the self-excited oscillation, will have a considerably

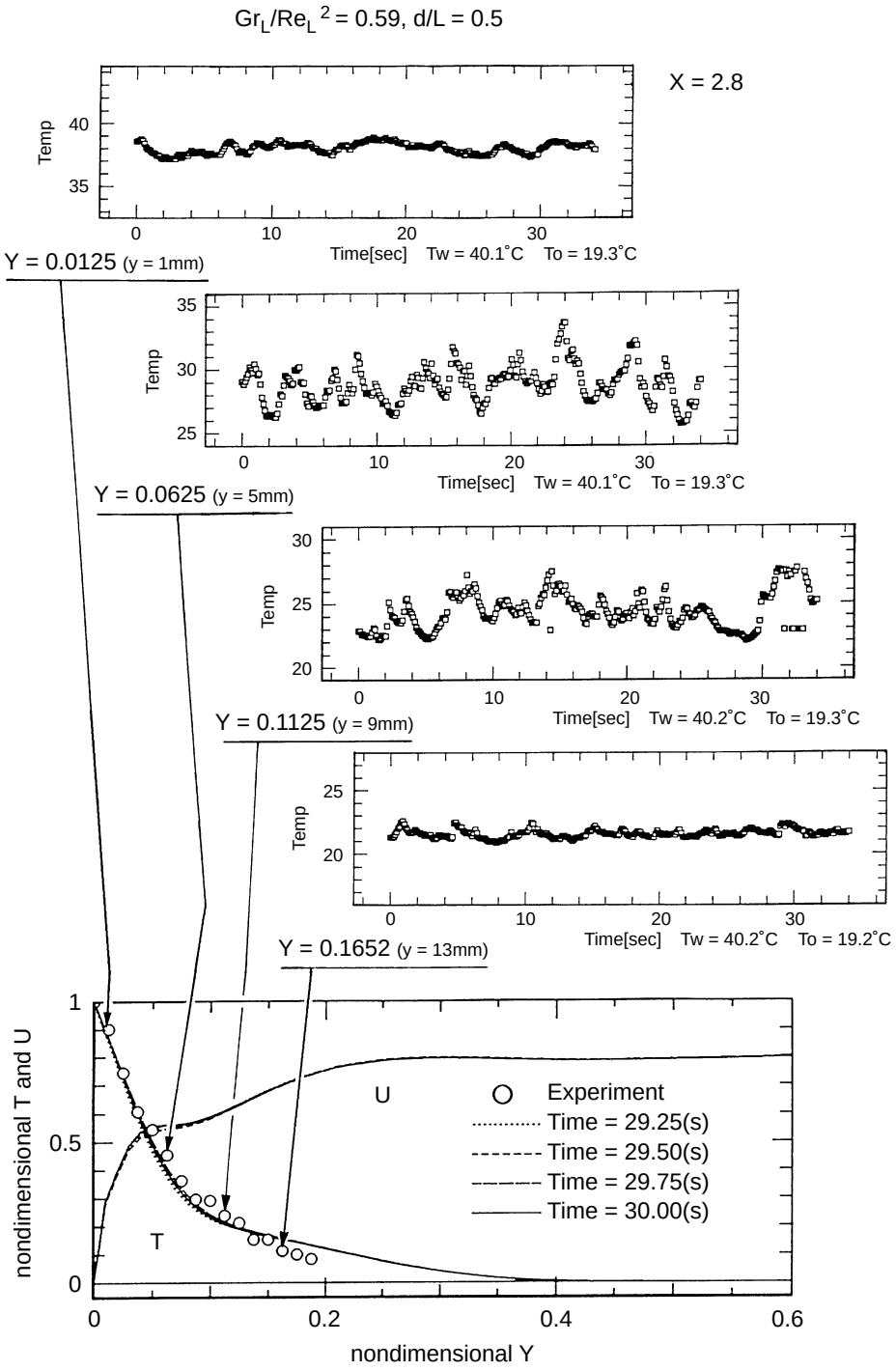


**Figure 15.**
Experimental verification of fluctuation of temperature field

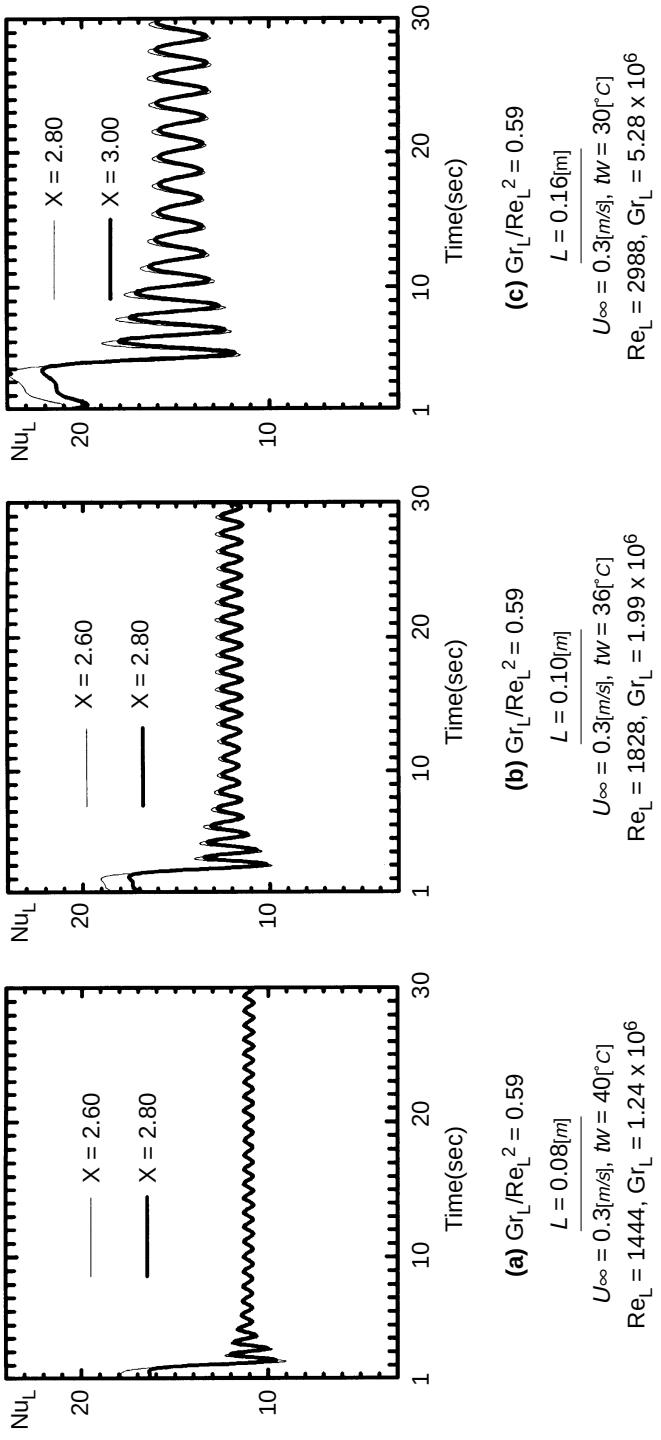


**Figure 16.**
Time history of unsteady fluctuating local Nusselt number $Nu_L$ for specified conditions of $Gr_L/Re_L^2$ = 0.59 and d/L = 0.5

different mode from each other depending on the Reynold number $Re_L$ in spite of the constant of $Gr_L/Re_L^2 = 0.59$. It is clear by the vorticity transport equation (5), that the parameter $Re_L$ plays an important role in the operating ratio between the viscosity force and the inertia and external forces, acting as the damping factor with decreasing in $Re_L$.

## 5. Conclusion

In this paper, a combined forced and free laminar convective heat transfer from an isothermally heated vertical plate with the backward-facing step was studied by the numerical calculation and experiment for a wide range of thermal conditions. The characteristic behavior of this mixed convection heat transfer, including the vortex flow in the recirculating region and the unstable fluctuation near the reattachment point, was clearly shown based on the numerical result and experiments by using the generalized coupling parameter of $Gr_L/Re_L^2$.

### References

Kishinami, K., Saito, H. and Suzuki, J. (1995), "A combined forced and free laminar convective heat transfer from a vertical plate with coupling of discontinuous surface heating", *Int. J. of Num. Meth. for Heat & Fluid Flow*, Vol. 5 No. 9, pp. 839-51.

Patankar, S.V. (1980), *Numerical Heat Transfer and Fluid Flow*, McGraw-Hill Corp., New York, NY.

Roache, P.J. (1976), *Computational Fluid Dynamics*, Hermora Publishers Inc.

Saito, H., Kishinami, K., Tokura, I. and Shinohara, M. (1995), "A study on natural convective heat transfer from a vertical plate followed by a backward step", *Proceedings of the 3rd ASME/JSME Thermal Engineering Joint Conference*, No.10309A, pp. 191-8.

Tsou, F.K., Chen, S.J. and Aung, W. (1991), "Starting flow and heat transfer downstream of a backward-facing step", *Trans. of the ASME, Journal of Heat Transfer*, Vol. 113, pp. 583-9.